methods

Quantification of sphingosine and sphinganine from crude lipid extracts by HPLC electrospray ionization tandem mass spectrometry

Bernd Lieser,[1] Gerhard Liebisch,[1] Wolfgang Drobnik, and Gerd Schmitz[2]

Institute for Clinical Chemistry and Laboratory Medicine, University of Regensburg, D-93042 Regensburg, Germany

Abstract **Sphingosine (SPH) comprises the backbone of sphingolipids and is known as a second messenger involved in the modulation of cell growth, differentiation, and apoptosis. The currently available methods for the quantification of SPH are, in part, complicated, time-consuming, insensitive, or unselective. Therefore, a fast and convenient methodology for the quantification of SPH and the biosynthetic intermediate sphinganine (SPA) was developed. The method is based on an HPLC separation coupled to electrospray ionization tandem mass spectrometry (MS/MS). Quantitation is achieved by the use of a constant concentration of a non-naturally occurring internal standard, 17-carbon chain SPH (C17-SPH), together with a calibration curve established by spiking different concentrations of naturally occurring sphingoid bases. SPH and SPA coeluted with C17-SPH, which allows an accurate correction of the analyte response. Interference of the SPH+2 isotope with SPA quantification was corrected by an experimentally determined factor. The limits of detection were 9 fmol for SPH and 21 fmol for SPA. The overall coefficients of variation were 8% and 13% for SPH and SPA, respectively. The developed HPLC-tandem mass spectrometry methodology, with an analysis time of 3.5 min, simple sample preparation, and automated data analysis, allows high-throughput quantification of sphingoid bases from crude lipid extracts and is a valuable tool for studies of cellular sphingolipid metabolism and signaling.**—Lieser, B., G. Liebisch, W. Drobnik, and G. Schmitz. **Quantification of sphingosine and sphinganine from crude lipid extracts by HPLC electrospray ionization tandem mass spectrometry. *J. Lipid Res.* 2003.** 44: **2209–2216.**

Supplementary key words high-performance liquid chromatography • sphingolipids • metabolism • high throughput

Sphingolipids, i.e., ceramide (CER), sphingosine-1-phosphate (SPP), and sphingosine (SPH) are known as important signaling molecules involved in the modulation of cell growth, differentiation, and apoptosis (1–3). In a cell type-specific manner, SPH has been shown to mediate pro- or antimitogenic effects (4, 5) and to regulate the activity of various signaling enzymes, including phospholipase D, diacylglycerol kinase, and protein kinase C (1, 2). In mammalian cells, SPH, with 18 carbon atoms and a *trans* double bond at position 4, comprises the backbone of more complex sphingolipid molecules. Sphinganine (SPA), which lacks the double bond, is an intermediate of sphingolipid biosynthesis without a known signaling function.

The existing detection methods for sphingoid bases involve different derivatization steps in order to enable quantification of the low cellular concentrations. A commonly used method established by Merrill et al. (6, 7) utilizes HPLC with fluorescence detection after ortho-phthaldialdehyde (OPA) derivatization of SPH and SPA. Other procedures are based on the conversion of SPH to radioactive derivates. Thus, SPH can be acetylated by [^{3}H]acetic-anhydride to *N*-[^{3}H]acetyl-SPH, which is separated by TLC, scraped, and analyzed by liquid scintillation counting (8). Other enzymatic methods include SPH kinase-mediated conversion of SPH to [^{32}P]SPP, followed by TLC separation and autoradiography (9, 10) or the conversion of SPH to C6-CER, with subsequent generation of C6-CER-1-[^{32}P]phosphate by diacylglycerol-kinase (11). All of these methodologies based on SPH-derivatization are multistep procedures, which are, in part, complicated or time consuming and therefore of limited value for high-throughput analysis.

As an alternative approach, mass spectrometry, as a highly sensitive and selective methodology, has been ap-

Abbreviations: CER, ceramide; C17-SPH, 17-carbon chain sphingosine; CV, coefficient of variation; ESI, electrospray ionization; FB1, fumonisin B1; IS, internal standard; MS/MS, tandem mass spectrometry; OPA, ortho-phthaldialdehyde; SPA, sphinganine; SPH, sphingosine; SPP, sphingosine-1-phosphate.

[1] B. Lieser and G. Liebisch contributed equally to this work.

[2] To whom correspondence should be addressed.
e-mail: gerd.schmitz@klinik.uni-regensburg.de

Manuscript received 9 July 2003 and in revised form 25 July 2003.

Published, JLR Papers in Press, August 1, 2003.
DOI 10.1194/jlr.D300025-JLR200

plied for SPH quantification. Two methods have been described that involve an HPLC separation prior to tandem mass spectrometric detection (LC-MS/MS) (12, 13). One protocol, published by Mano et al. (12), used *N*-acetyl-SPH (C2-CER) as internal standard (IS) and allowed the simultaneous analysis of several sphingolipids within a total run time of 15 min. Sullards et al. (13) described the separation of SPH, SPA, and their corresponding 1-phosphates within a run time of 13 min. Recently, Seefelder et al. (14) presented a methodology for quantification of SPH and SPA without lipid extraction prior to LC-mass spectrometry (LC-MS) analysis. Phytosphingosine was used as IS, and the methodology showed a total run time of 14 min.

The aim of the present study was to develop a simple and fast methodology based on the high sensitivity and selectivity of electrospray ionization-tandem mass spectrometric (ESI-MS/MS) for the quantification of SPH and SPA that is applicable for high-throughput analysis.

MATERIALS AND METHODS

Materials

17-Carbon chain SPH (C17-SPH), SPH, and SPA were obtained from Avanti Polar Lipids (Alabaster, AL). Methanol and chloroform were of HPLC grade, purchased from Merck KG (Darmstadt, Germany) and J. T. Baker (Gross-Gerau, Germany). Formic acid was of analytical grade and was purchased from Merck KG.

Cell culture

Fibroblasts were cultured in Dulbecco's modified Eagle's medium (DMEM) supplemented with L-glutamine, nonessential amino acids, and 10% fetal calf serum (FCS) in a humidified 5% CO_2 atmosphere at 37°C, and confluent cells were used for the experiments. Other cell types were cultured according to American Type Culture Collection recommendations. Adherent cell types were cultured to confluence, and suspension cells were grown to the recommended cell density before analysis.

Sample preparation

Cells were rinsed two times with ice-cold phosphate-buffered saline (PBS) and scraped in PBS. After centrifugation at 240 *g* for 7 min, the resulting pellet was homogenized in distilled water by sonication. An aliquot was taken for protein determination. C17-SPH was added as IS (175 ng per mg of cellular protein). Lipids were extracted according to the method of Bligh and Dyer (15). The dried lipid extracts were resolved in the mobile phase. Calibration lines were generated by adding different amounts of naturally occurring SPH and SPA to cell homogenates.

LC-MS/MS

Samples were quantified by LC-MS/MS. A Waters Alliance 2790 (Milford, MA) was used with a constant flow of 300 μl/min and a mobile phase of methanol-chloroform (3:1; v/v) containing 0.1% (v) formic acid. The HPLC column was a Thermo Hypersil-Keystone Beta Basic CYANO, 3 μm, 50 × 2 mm (Kleinostheim, Germany). The injection volume was 5 μl, and the column temperature was set to 30°C. The triple quadrupole mass spectrometer (Quattro Ultima, Micromass, Manchester, UK) was operated with the following settings: capillary voltage, 3 kV; cone voltage, 35 V; collision energy, 14 V; and a collision gas pressure of 1.75e-3 Torr argon.

The mass resolution for quadrupole 1 and quadrupole 3 was above unit resolution. The mass spectrometer was operated in multiple reaction monitoring modus monitoring the following transitions: m/z 300 > 282, 300 > 264, and 300 > 252 for SPH; 302 > 284, 302 > 266, and 302 > 254 for SPA; and 286 > 268, 286 > 250, and 286 > 238 for C17-SPH. Data analysis was performed with MassLynx software (Micromass) coupled to self-programmed Excel macros. The SPA peak area was corrected for the overlap resulting from the M+H+2 isotope peak of SPH. The percentage overlap was determined within each run by a triplicate injection of an SPH standard. The theoretical overlap of the 300 > 282 transition with the 302 > 284 transition was calculated using the MassLynx Mass Calculator.

Protein determination

Protein concentrations were measured according to the method of Smith et al. (16).

RESULTS

Fragmentation

In analogy to the published mass spectrometric methodologies (12–14), ESI in the positive-ion mode was used for SPH analysis. The product ion spectrum of SPH (**Fig. 1**) showed fragments of m/z 282, 264, and 252 resulting from a loss of one water molecule ($-H_2O$), two water molecules ($-2H_2O$), and one water and formaldehyde molecule ($-H_2O$-HCHO), respectively. The hydrogenated biosynthetic intermediate SPA exhibited an identical fragmentation pattern, with fragments of m/z 284, 266, and 254. Similarly, the non-naturally occurring C17-SPH, which was used as IS, exhibited collision-induced fragments of m/z 268, 250, and 238. The most intense fragment of these sphingoid bases results from the loss of one water at an optimal collision energy of 14 V and a collision gas pressure of 1.75e-3 Torr. The collision-induced loss of two water or of one water plus formaldehyde needs a slightly higher collision energy of 15–16 V to yield maximum signal intensities.

HPLC separation

First, we tried to use these transitions for a direct quantification of SPH by flow injection of crude lipid extracts from fibroblasts. However, this approach did not yield acceptable signals, probably reflecting signal suppression by other components of the crude lipid extract. In order to further clarify this issue, a fixed amount of C17-SPH was measured by direct flow injection, either pure or in a crude fibroblast lipid extract matrix. The comparison of signal intensities revealed a suppression of about 70% in the lipid matrix (data not shown). In order to reduce this suppressive effect, we decided to establish an HPLC separation for sphingoid bases, with a short run time and a coelution of analytes and IS. The latter is of major importance, because only a coelution of analytes and IS ensures an accurate compensation for possible ionization interferences or machine instabilities. A cyanopropyl material was used as stationary phase, and the mobile phase was methanol-chloroform (3:1; v/v), with formic acid as ionization additive. The concentration of formic acid had great in-

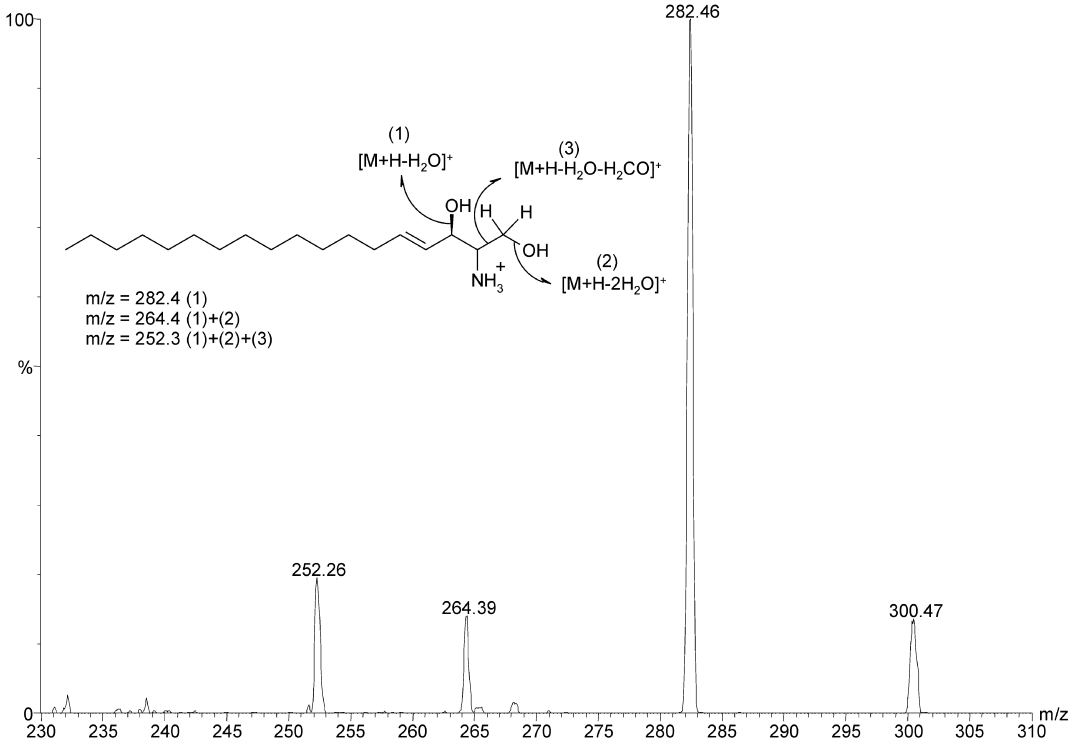

Fig. 1. Product ion spectrum of an authentic sphingosine (SPH) standard and fragmentation scheme for SPH (M = 299 g/mol).

fluence on the sphingoid base retention time as well as on the ionization efficiency (**Table 1**); 0.05% compared with 0.025% formic acid increased the SPH peak area by ~50%, but had only a minor effect on the retention time. A further doubling of formic acid concentration to 0.1% reduced the retention time significantly, to 2.65 min (**Fig. 2**), but did not induce a further increase of signal intensity (Table 1). Using 0.1% formic acid as ionization additive, other phospholipids, such as phosphatidylcholine, sphingomyelin, phospatidylethanolamine, and phosphatidylserine, were clearly separated from the sphingoid bases (Fig. 2). Furthermore, comparison of IS signal intensity injected without lipid matrix and spiked to crude fibroblast lipid extract revealed no signal suppression (data not shown). Therefore, a mobile phase of methanol-chloroform (3:1; v/v) containing 0.1% formic acid was selected for further experiments. The use of crude lipid extracts had no negative effect on the stability of the HPLC column, with a lifetime of more than 1,000 injections and without any cleaning step (data not shown).

Three transitions were monitored for SPH, C17-SPH, and SPA. The loss of one molecule of water ($-H_2O$) showed the highest intensity, followed by the loss of two water and formaldehyde molecules ($-H_2O$-HCHO; ~12% of the $-H_2O$ transition for SPH), and the loss of two water molecules ($-2H_2O$; ~10% of the $-H_2O$ transition for SPH). The intensities of all three transitions were sufficient for the analysis of fibroblast SPH levels. However, at equal concentrations, SPA exhibited only one-third the signal intensity of SPH. In addition, cellular SPA concentrations are typically lower than SPH concentrations. Therefore, only the intensities of the $-H_2O$ transition were suitable for the quantification of cellular SPA levels.

Quantification

In order to compensate for variations in sample preparation and ionization efficiency, C17-SPH, a non-naturally occurring species, was added as IS prior to lipid extraction. The ratio between analyte and IS peak area was used for quantification.

Due to the coelution of SPH and SPA, an overlap existed between the SPH+2 isotope peak (*m/z* 302) and the SPA transition 302 > 284. To address this issue, the percentage of overlap was experimentally determined by injection of pure SPH standard within each run. Typically, values of ~2.5% were found, which is close to the theoret-

TABLE 1. Influence of the formic acid concentration on the response and retention time of sphingoid bases

Formic Acid Concentration	Retention Time	Area SPH
%	*min*	
0.025	4.29	21,000
0.05	4.00	32,500
0.1	2.65	34,500

SPH, sphingosine. The percentage of formic acid in the mobile phase consisting of methanol-chloroform (3:1; v/v) was increased from 0.025% to 0.1%. The table shows the respective retention times of sphingoid bases and the peak areas of the SPH-H_2O transition (*m/z* 300 > 282) measured in fibroblast lipid extracts.

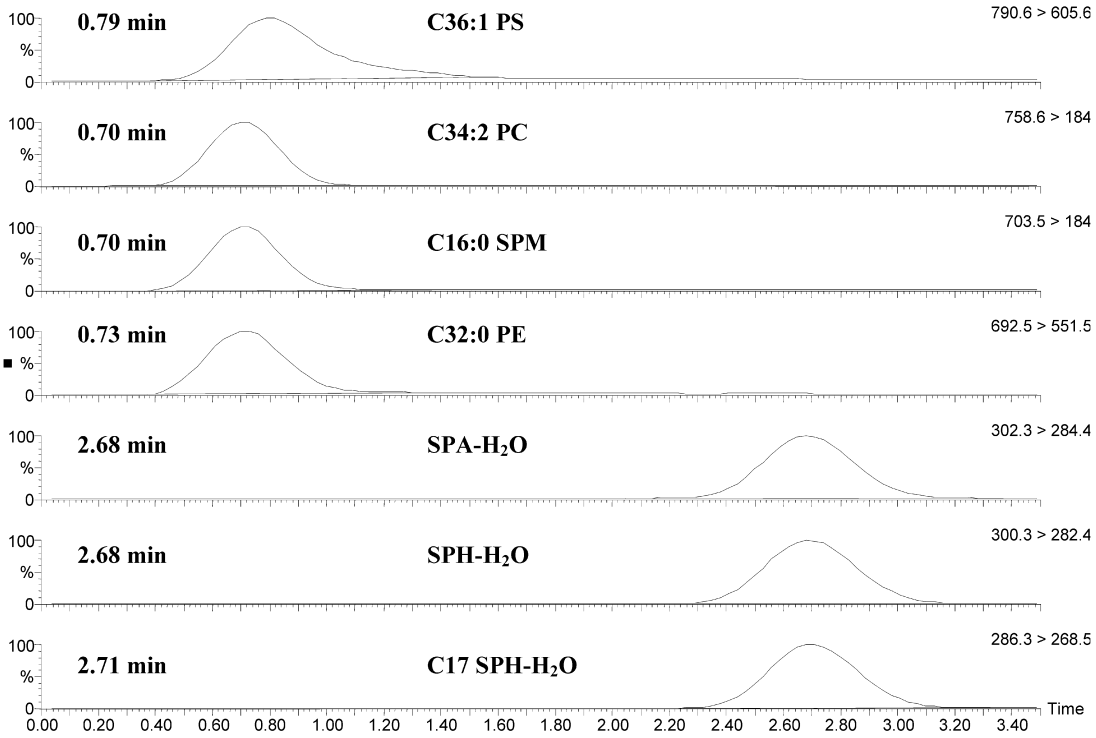

Fig. 2. Chromatogram of crude fibroblast lipid extract corresponding to 1.75 μg cellular protein on column. Displayed are tandem mass spectrometry transitions representative of distinct phospholipid classes and the sphingoid bases SPH, sphinganine (SPA), and internal standard (IS) 17-carbon chain SPH (C17-SPH) with their respective retention times: C36:1-phosphatidylserine [C36:1 PS (*m/z* 790 > 605)]; C34:2-phosphatidylcholine [C34:2 PC (*m/z* 758 > 184)]; C16:0-sphingomyelin [C16:0 SPM (*m/z* 703 > 184)]; C32:0 phosphatidylethanolamine [C32:0 PE (*m/z* 692 > 551)]; SPA-H_2O (*m/z* 302 > 284); SPH-H_2O (*m/z* 300 > 282); and C17-SPH-H_2O (*m/z* 286 > 268).

ically calculated value of 2.29%. The experimentally measured value was used to correct peak intensity of the 302 > 284 transition. This approach was validated by the addition of SPH to a fibroblast homogenate, which did not result in an increase of SPA concentration after overlap correction (**Table 2**).

Calibration lines were generated by the addition of different concentrations of naturally occurring SPH and SPA to cell homogenates (**Fig. 3**). The obtained standard curves were linear in the tested range, and the 300 > 282 transition ($-H_2O$) typically showed the highest slope, compared with the other monitored SPH transitions, 300 > 264 ($-2H_2O$) and 300 > 252 ($-H_2O$-HCHO). Quantitative values calculated from standard curves using the different SPH transitions were very similar (**Table 3**). The slope of the standard curve for SPA quantification using the 302 > 284 transition was 40% that of the SPH calibration line.

Additionally, we investigated whether the slopes of the calibration lines differed depending on cell type. Calibration lines were generated with equal amounts of cellular protein from control and Tangier disease fibroblasts, HELA cells, and primary human keratinocytes. The resulting calibration line slopes were not significantly different. The coefficients of variation (CVs) of the calibration line slopes using different cell types were: 6.0% for 300 > 282, 7.7% for 300 > 264, and 8.5% for 300 > 252 (SPH transitions); and 7.4% for SPA.

Recovery and limit of detection

SPH recovery was tested by the addition of 5–50 ng SPH prior to lipid extraction. The mean recovery was 92.0 ± 6.4%, and no correlation to the spiked amount was observed (data not shown).

For evaluating the limit of detection, an analyte-free matrix would be optimal, because particularly for ESI applications, the influence of matrix components has to be considered. However, because we did not detect any influence of sample matrix on sphingoid base signals after HPLC separation, it may be acceptable to use pure standard for determining the detection limit. Therefore we

TABLE 2. Isotope correction for SPA

Spike SPH	Ratio SPH/IS	Uncorrected Ratio SPA/IS	Corrected Ratio SPA/IS
ng			
0	0.107	0.0190	0.0163
5	0.337	0.0234	0.0151
15	1.030	0.0410	0.0156
25	1.705	0.0575	0.0155
50	3.438	0.1013	0.0165

IS, internal standard; SPA, sphinganine. A crude fibroblast cell homogenate was spiked with increasing amounts of SPH. Values represent ratios of peak areas of SPH or SPA relative to the IS 17-carbon chain sphingosine. The SPA-to-IS ratio is shown uncorrected as well as after correction of the SPA peak area as described in Materials and Methods.

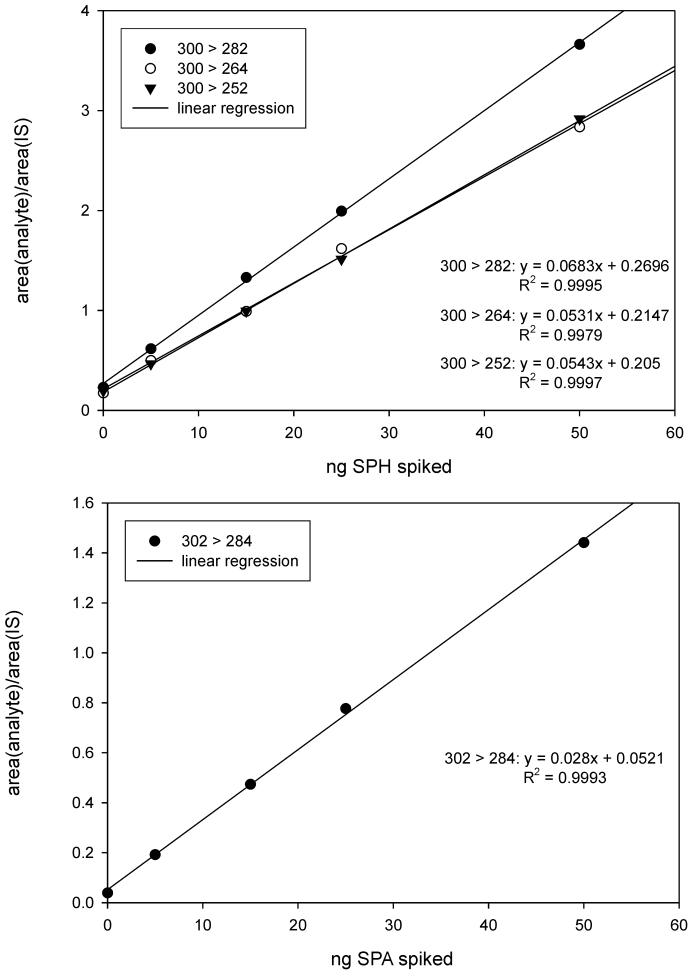

Fig. 3. Calibration lines for SPH and SPA. Calibration lines were established from fibroblast cell homogenates by the addition of SPH and SPA prior to lipid extraction (n = 1). For each calibration level, cell homogenate corresponding to 175 μg cellular protein was used. The plots show the peak area ratio of analyte to C17-SPH (IS) relative to the spiked amount of SPH/SPA. Regression lines were generated by linear least-square fit. Three transitions are displayed for SPH (upper panel): SPH-H_2O (closed circles), m/z 300 > 282; SPH-$2H_2O$ (open circles), m/z 300 > 264; and SPH-H_2O-HCHO (triangles), m/z 300 > 252. The SPA-H_2O m/z 302 > 284 transition is shown for SPA (lower panel). The equation of the regression line and the regression coefficient are displayed for each transition.

used authentic standards to assess the limit of detection, defined as a peak with a signal-to-noise ratio above three. The observed detection limits for SPH (300 > 282) and SPA were 9 fmol and 21 fmol, respectively. If SPH quantification was based on the transitions 300 > 264 and 300 > 252, the detection limit was ~25 fmol.

Interday and intraday precision

The precision of the developed assay was assessed with fibroblast samples. The intraday CV was below 6% for all transitions monitored (Table 3), with the best precision for the 300 > 282 SPH transition, showing a CV of 2.8%. For SPA, an intraday CV of 4.4% was observed. Similarly, the best interday CV of 7.6% was observed for the 300 > 282 transition. For SPA, the total CV was ~13%.

Sample stability

In order to investigate sample stability, sphingoid base concentrations of a fibroblast cell homogenate were measured immediately, after 4 h, and after 24 h at room temperature (**Table 4**). After 4 h and 24 h at room temperature, SPH and SPA concentrations were increased by ~20% and ~80%, compared with the freshly analyzed sample, respectively. Immediately frozen samples did not differ in sphingoid base levels compared with freshly analyzed cell homogenates (data not shown).

Cellular sphingoid base level

Primary human fibroblasts cultured in DMEM supplemented with 10% FCS showed SPH and SPA concentrations in the range of 50 to 200 pmol/mg and 10 to 60 pmol/mg, respectively (data not shown). Similar SPH and SPA concentrations were found for the mouse fibroblast cell line NIH 3T3 cultured in FCS medium (**Table 5**). Eighteen hours after a culture medium change to 0.2% BSA, the SPH concentration decreased, whereas the SPA levels increased. Consequently, the SPH-to-SPA ratio declined from 2.7 in the presence of FCS to 1.5 in the ab-

TABLE 3. Interday and intraday precision

	m/z 300 > 282, 302 > 284		m/z 300 > 264		m/z 300 > 252	
n = 10	Mean	CV	Mean	CV	Mean	CV
	pmol/mg cell protein					
Interday SPH	98.9	7.6	96.2	11.5	96.2	10.6
Interday SPA	33.5	12.8				
Intraday SPH	76.1	2.8	75.9	5.6	75.6	5.0
Intraday SPA	38.1	4.4				

CV, coefficient of variation. Ten samples from pooled fibroblast cell homogenates were analyzed, either in one run for intraday precision or in different runs for interday precision.

TABLE 4. Stability of cell homogenates

Time at Room Temperature	SPH	SPA
h	*pmol/mg cell protein*	
0	161	18
4	196	23
24	284	34

Cell homogenates of primary fibroblast cultures were analyzed immediately or allowed to stand for 4 h and 24 h at room temperature before analysis.

sence of FCS. Under both conditions, the CER synthase inhibitor fumonisin B1 (FB1) (17) induced only a slight increase in cellular SPH concentrations of 25% to 30%. In contrast, FB1 treatment increased SPA concentrations by >100% in medium containing FCS and by ~50% in medium containing BSA (Table 5). Confluent primary human keratinocytes showed sphingoid base levels comparable to those of fibroblasts, with 180 pmol/mg for SPH and 60 pmol/mg for SPA. In contrast, the leukocyte cell lines HL60 and U937 showed significantly lower sphingoid base levels. The SPH concentrations in HL60 and U937 cells were 11 pmol/mg and 14 pmol/mg, respectively (Table 5).

DISCUSSION

SPH has been described as a modulator of several cellular targets, including protein kinase C, diacylglycerol kinase, and phospholipase D (1–3). Concerning the biological function of SPH, several conflicting results exist, especially for the role of SPH in the regulation of cell growth (4, 5). These controversial data may be related to a fast conversion of SPH into other sphingolipid metabolites, including CER and SPP, which have, in part, opposite signaling activity (2, 3). Therefore, it is of relevance to assess a profile of different sphingolipids, instead of one single metabolite. Such an approach would require the combination of several conventional methodologies, with a high demand of time and material. Moreover, only some of the existing conventional procedures for SPH quantification enable a differentiation of bioactive SPH from the biosynthetic intermediate, SPA. In particular, procedures based on a conversion of SPH into radioactive products also convert SPA, and the subsequent TLC separation cannot clearly resolve the SPH from the SPA derivative (8–11). A commonly applied HPLC method by Merrill et al. (6, 7) is able to differentiate between SPH and SPA, but has limitations concerning the rather long run time of ~20 min and the required OPA derivatization. In contrast to these conventional methodologies, mass spectrometry offers advantages because of its high sensitivity and selectivity, and may serve as platform for sphingolipid profiling. Several methodologies for mass spectrometric SPH analysis have already been described, and all of these methods use C18 reversed-phase HPLC columns for the separation of the sphingolipid analytes (12–14). Because these columns usually separate the analyte from the IS, an accurate correction of possible interferences with the ESI process or of machine instabilities is not ensured.

The method of Mano et al. (12) allows the quantification of several different sphingolipids; however, C2-CER was used as IS for SPH quantification. This could be a potential source of error, because CER clearly differs in its chemical structure from SPH and shows a different ionization and fragmentation behavior. A second study by Sullards (13) applies as IS C20-SPH, which occurs naturally (18) and which may disturb the analysis. In addition, the paper does not include data concerning precision and detection limits, and leaves unclear whether the IS coelutes with the analytes. Therefore, a detailed comparison with the method described in this manuscript is not possible. A recently published methodology by Seefelder et al. (14) uses LC-MS for SPH and SPA quantification without prior lipid extraction. This methodology has a total run time of 14 min, and SPH shows a partial chromatographic overlap with the IS phytoSPH, but both are clearly separated from SPA. Although their study was performed with a triple quadrupole mass spectrometer, fragment analysis was not used to improve specificity. This may possibly be due to signal-suppressing matrix effects from the injected crude sample, resulting in a low sensitivity, which does not permit the analysis of molecule fragments.

The aim of the current study was to establish a fast and simple quantitative detection method for SPH and SPA from crude lipid extracts using ESI-MS/MS. Because quantification of sphingoid bases by direct flow injection

TABLE 5. Cellular level of SPH and SPA

Cell Type	Culture Medium	SPH	SPA
		pmol/mg cell protein	
NIH 3T3	10% FCS	127 ± 14	47 ± 5
	10% FCS + 25 μM FB1	157 ± 15	102 ± 7
	0.2% BSA	90 ± 10	64 ± 2
	0.2% BSA+ 25 μM FB1	118 ± 12	99 ± 14
HL60	10% FCS	11.1 ± 1.0	2.5 ± 0.3
U937	10% FCS	14.3 ± 1.0	5.5 ± 0.7
Human primary keratinocytes	Keratinocyte growth medium	177 ± 18	58 ± 5

FB1, fumonisin B1; FCS, fetal calf serum. All adherent cells were grown to confluence and incubated in the indicated culture medium for 18 h before analysis. HL60 and U937 cells were cultured for 18 h at a density of 2 million cells/ml. The displayed values represent mean ± SD from one experiment measured in triplicate.

analysis was prevented by high signal suppression, a fast HPLC methodology with a clear separation between sphingoid bases and other major phospholipids was developed. The signal suppression for sphingoid bases was completely eliminated, and correction for possible interferences with ionization and fragmentation as well as for machine instabilities was ensured by the coelution of the IS with SPH and SPA. C17-SPH should be superior, compared with the IS used in other mass spectrometric methods, because it is a non-naturally occurring analog and differs only by one methylen group from the main mammalian SPH species, C18-SPH. In contrast to already-existing MS/MS methods, which use only the collisional-induced loss of water, two additional transitions were monitored for SPH quantification. Linear calibration lines for SPH and SPA were generated by the addition of standards, and these calibration lines were independent of the cellular matrix, allowing the use of one single calibration line for samples from different cell types. Cellular SPH concentrations calculated from standard curves based on the three different transitions were similar (Table 3), supporting the high specificity of the method. For SPA, only the collision-induced loss of water delivers a signal intensity sufficient to monitor cellular concentrations; this is due primarily to the reduced ionization efficiency of SPA compared with SPH. This phenomenon may be related to a reduced charge stabilization because of the missing double bond in SPA. Moreover, cellular SPA concentrations are commonly lower than those of SPH (Table 5).

Because the SPH+2 isotope interferes with SPA quantification, SPA measurements were corrected by an experimentally determined overlap factor, which is similar to the theoretically calculated value (Table 2). This factor should be determined within each run, because it may be influenced by mass calibration and the resolution of the mass spectrometer.

The applied simple, one-step lipid extraction showed almost complete recovery of SPH, and removed protein and hydrophilic contaminants from the sample. Thus, after more than 1,000 injections, no significant changes of analyte peak shape or signal intensity were observed (data not shown). The methodology showed an excellent in-run precision, with a CV below 6% for all monitored transitions and a total CV below 13%. For SPH, the highest precision was obtained for the $300 > 282$ transition, which may be due to the higher calibration line slope and signal intensity of this transition, compared with those of $300 > 264$ and $300 > 252$ (Fig. 3). As a consequence, the $300 > 282$ transition shows a significantly lower detection limit, compared with the other SPH transitions. Therefore, this transition should be used for SPH quantification, whereas the $300 > 264$ and $300 > 252$ transitions could serve as an internal quality check. The achieved detection limit was significantly lower, compared with that of already-published methodologies for SPH quantification. Thus, Ohta et al. (8) described a working range down to 10 pmol for a radioactive acetylation assay. Twenty-five picomoles as the lower limit of quantitation was reported for an assay applying a combination of chemical and enzymatic conversion by Van Veldhoven et al. (11), as well as for an SPH kinase-mediated generation of radioactive SPP (10).

Sphingoid base levels were analyzed in several different cell types, and significant differences were observed. Compared with fibroblasts and keratinocytes, the leukocyte cell lines HL60 and U937 were characterized by lower sphingoid base concentrations. In accordance with our findings, Ohta et al. (8) reported ~4-fold higher SPH levels in a gastric cancer cell line, compared with HL60 and U937 leukemia cell lines. This study used a derivatization-based methodology, with conversion of SPH into radioactive C2-CER, and reported SPH concentrations of 6.3 pmol/10^6 cells for HL60 and 6.8 pmol/10^6 cells for U937. We found SPH concentrations of 11.1 and 14.3 pmol/mg cell protein in HL60 and U937 cells, respectively. Related to cell numbers, the concentrations were 1.4 pmol/10^6 HL60 cells and 1.9 pmol/10^6 U937 cells (data not shown). The higher concentrations found by Ohta et al. may, in part, arise from methodological differences, because their method did not differentiate between SPH and SPA. Alternatively, such differences may also result from different cell culture conditions, as has been suggested by previous publications (19, 20). Indeed, we observed a great difference in sphingoid base levels for NIH 3T3 fibroblasts cultured in medium containing either 10% FCS or 0.2% BSA. However, another study using MS/MS (12) reported SPH concentrations of 2.0 pmol/10^6 HL60 cells, which is in good accordance with our value. In HACAT cells, Min et al. (7) showed an SPH concentration of 230 pmol/mg and an SPA concentration of 110 pmol/mg using OPA derivatization and HPLC analysis. These data are similar to the sphingoid base levels in primary human keratinocytes as measured in the present study (Table 5).

Further evidence for the validity of the developed methodology derives from the observed increase of sphingoid base levels after treatment of NIH 3T3 fibroblasts with the CER synthase inhibitor FB1 (Table 5) (17). The more-pronounced increase of cellular SPA compared with SPH concentrations maybe due to a more active sphingolipid biosynthesis compared with SPH reacylation or a higher inhibitory effect of FB1 on sphingolipid biosynthesis.

In summary, all of these data support the validity of the developed ESI-MS/MS method. In contrast to already existing protocols, the assay offers advantages with respect to simple sample preparation, a short analysis time of 3.5 min per sample, as well as the ruggedness and sensitivity of the measurement. These features, coupled with highly automated data processing software, make this methodology a valuable tool for investigating the metabolism and signaling of sphingolipids.

This work was supported by Deutsche Forschungsgemeinschaft (DFG DR 348/2-2) (W.D.).

REFERENCES

1. Gomez-Munoz, A. 1998. Modulation of cell signalling by ceramides. *Biochim. Biophys. Acta.* **1391:** 92–109.

2. Hannun, Y. A., C. Luberto, and K. M. Argraves. 2001. Enzymes of sphingolipid metabolism: from modular to integrative signaling. *Biochemistry.* **40:** 4893–4903.
3. Huwiler, A., T. Kolter, J. Pfeilschifter, and K. Sandhoff. 2000. Physiology and pathophysiology of sphingolipid metabolism and signaling. *Biochim. Biophys. Acta.* **1485:** 63–99.
4. Maceyka, M., S. G. Payne, S. Milstien, and S. Spiegel. 2002. Sphingosine kinase, sphingosine-1-phosphate, and apoptosis. *Biochim. Biophys. Acta.* **1585:** 193–201.
5. Merrill, A. H., Jr., E. M. Schmelz, D. L. Dillehay, S. Spiegel, J. A. Shayman, J. J. Schroeder, R. T. Riley, K. A. Voss, and E. Wang. 1997. Sphingolipids—the enigmatic lipid class: biochemistry, physiology, and pathophysiology. *Toxicol. Appl. Pharmacol.* **142:** 208–225.
6. Merrill, A. H, Jr., E. Wang, R. E. Mullins, W. C. Jamison, S. Nimkar, and D. C. Liotta. 1988. Quantitation of free sphingosine in liver by high-performance liquid chromatography. *Anal. Biochem.* **171:** 373–381.
7. Min, J. K., H. S. Yoo, E. Y. Lee, W. J. Lee, and Y. M. Lee. 2002. Simultaneous quantitative analysis of sphingoid base 1-phosphates in biological samples by o-phthalaldehyde precolumn derivatization after dephosphorylation with alkaline phosphatase. *Anal. Biochem.* **303:** 167–175.
8. Ohta, H., F. Ruan, S. Hakomori, and Y. Igarashi. 1994. Quantification of free sphingosine in cultured cells by acylation with radioactive acetic anhydride. *Anal. Biochem.* **222:** 489–494.
9. Edsall, L. C., and S. Spiegel. 1999. Enzymatic measurement of sphingosine 1-phosphate. *Anal. Biochem.* **272:** 80–86.
10. Olivera, A., J. Rosenthal, and S. Spiegel. 1994. Sphingosine kinase from Swiss 3T3 fibroblasts: a convenient assay for the measurement of intracellular levels of free sphingoid bases. *Anal. Biochem.* **223:** 306–312.
11. Van Veldhoven, P. P., W. R. Bishop, and R. M. Bell. 1989. Enzymatic quantification of sphingosine in the picomole range in cultured cells. *Anal. Biochem.* **183:** 177–189.
12. Mano, N., Y. Oda, K. Yamada, N. Asakawa, and K. Katayama. 1997. Simultaneous quantitative determination method for sphingolipid metabolites by liquid chromatography/ionspray ionization tandem mass spectrometry. *Anal. Biochem.* **244:** 291–300.
13. Sullards, M. C. 2000. Analysis of sphingomyelin, glucosylceramide, ceramide, sphingosine, and sphingosine 1-phosphate by tandem mass spectrometry. *Methods Enzymol.* **312:** 32–45.
14. Seefelder, W., G. Schwerdt, R. Freudinger, M. Gekle, and H. U. Humpf. 2002. Liquid chromatography/electrospray ionisation-mass spectrometry method for the quantification of sphingosine and sphinganine in cell cultures exposed to fumonisins. *J. Chromatogr. B Analyt. Technol. Biomed. Life Sci.* **780:** 137–144.
15. Bligh, E. G., and W. J. Dyer. 1959. A rapid method of total lipid extraction and purification. *Can. J. Med Sci.* **37:** 911–917.
16. Smith, P. K., R. I. Krohn, G. T. Hermanson, A. K. Mallia, F. H. Gartner, M. D. Provenzano, E. K. Fujimoto, N. M. Goeke, B. J. Olson, and D. C. Klenk. 1985. Measurement of protein using bicinchoninic acid. *Anal. Biochem.* **150:** 76–85. [Erratum. 1987. *Anal. Biochem.* **163:** 279.]
17. Desai, K., M. C. Sullards, J. Allegood, E. Wang, E. M. Schmelz, M. Hartl, H. U. Humpf, D. C. Liotta, Q. Peng, and A. H. Merrill, Jr. 2002. Fumonisins and fumonisin analogs as inhibitors of ceramide synthase and inducers of apoptosis. *Biochim. Biophys. Acta.* **1585:** 188–192.
18. Sonnino, S., and V. Chigorno. 2000. Ganglioside molecular species containing C18- and C20-sphingosine in mammalian nervous tissues and neuronal cell cultures. *Biochim. Biophys. Acta.* **1469:** 63–77.
19. Lavie, Y., J. K. Blusztajn, and M. Liscovitch. 1994. Formation of endogenous free sphingoid bases in cells induced by changing medium conditions. *Biochim. Biophys. Acta.* **1220:** 323–328.
20. Smith, E. R., and A. H. Merrill, Jr. 1995. Differential roles of de novo sphingolipid biosynthesis and turnover in the "burst" of free sphingosine and sphinganine, and their 1-phosphates and N-acyl-derivatives, that occurs upon changing the medium of cells in culture. *J. Biol. Chem.* **270:** 18749–18758.